

L03 KINETIC OF DEGRADATION OF HISTORICAL DOCUMENTS CONTAINING IRON-GALL INKS

MICHAL ČEPPAN, VIERA JANČOVIČOVÁ, MILENA REHÁKOVÁ and ANDREJ BUZINKAY

Faculty of Chemical and Food Technology, Slovak University of Technology, Radlinského 9, 812 37 Bratislava, michal.ceppan@stuba.sk

Introduction

Deterioration of paper documents containing iron-gall inks is supposed to be a combination of two degradation pathways – acid hydrolysis of cellulose and oxidative degradation of cellulose. Iron gall inks contain transition metals, such as iron and copper, catalyzing the radical oxidation of the substrate, as well as acids, catalyzing its hydrolysis^{1,2}. Transition metals are capable to enter Fenton and Fenton-like type of reactions^{3,4} and catalyze homolytic decomposition of peroxides with production of hydroxyl radicals. Hydroxyl radicals can oxidize cellulose and induce degradation of cellulose⁵.

Content and ratio of transition metals in historical iron-gall inks recipes vary. In addition to iron the most notable transition metal is cooper and the molar ration of the iron cooper to iron in these recipes get the value up to 0.7(ref.⁶). It was found that even trace amounts of cooper induce significant destruction of paper substrate⁷. The catalytic action of cooper in Fenton and Fenton-like reactions predominate over the catalytic action of iron^{6,8} and the catalytic action of iron and cooper is additive⁶.

The influence of transitional metals in iron-gall inks on the rate of degradation and change of optical properties of aged model documents were studied in this paper.

Experimental

Model ink systems were prepared according to the suggestion of Neevel². The molar ratio of transition metal:tannine (5.5:1) and the amount of gum arabic (4.71 g l50 ml⁻¹) were kept constant. Seven model inks with the ratio of copper:iron 0 (without cooper), 0.025, 0.05, 0.10, 0.25, 0.40 (A1–A6) and model ink containing only Cu without iron (A7) were used in this study. Used chemicals: tannic acid (Sigma Aldrich), ferric sulphate heptahydrate (Lachema, Czech Rep.), cupric sulphate pentahydrate (Lachema, Czech Rep.), gum arabic (Sigma-Aldrich), cupriethylene-diamine (Sigma-Aldrich), deionised water. Water solutions of inks were applied on substrate after 15 days free staying in dark.

Whatman filter paper No. 1 (purified cotton linter cellulose) was used as a model substrate. Using a computer-guided plotter with a refillable plotter pen each ink was applied in rectangles (12×5 cm) and then left to dry at room temperature. The average ink amount per sample was 0.008 g cm⁻². Samples with pH values lying in four different regions (~3, ~4, ~5, ~6) were obtained by short immersion (2–3 s) of inked paper samples into the diluted solutions of sodium hydroxide (from 0.25M to 0.40M, as appropriate for particu-

lar sample to obtain required pH)). The samples were submitted to accelerated ageing in closed vessels at 90 °C according to the method described by Lojewski and Baranski⁹.

The degree of polymerization (DP) of samples was determined viscometrically using cupriethylene-diamine as a solvent¹⁰. Degree of polymerization was calculated from viscometric data using Mark-Houwink-Sakurada equation and the constants according to Evans and Wallis^{11,12}. Rate constants “k” of degradation of paper samples was calculated by least squares fitting of the plot DP vs. time using Ekenstam equation for degradation of linear polymers¹³:

$$(1/DP_t) = (1/DP_0) + k t \quad (1)$$

where DP_t and DP₀ are degrees of polymerization at the beginning of ageing and after time “t” of ageing, respectively.

Colorimetric measurements were performed using spectrophotometer GretagMacbeth Spectrolino keeping the standard condition for graphic arts measurements (geometry 45/0, D50 illumination, 2° standard observer, measurement without polarizing filter, black background) according to the standard¹⁴. Standard error of the colorimetric measurements was less than 1.0 (in ΔE_{ab}^*).

Results and Discussion

The rates constants of degradation of samples containing model inks at various pH are shown on the Fig. 1.

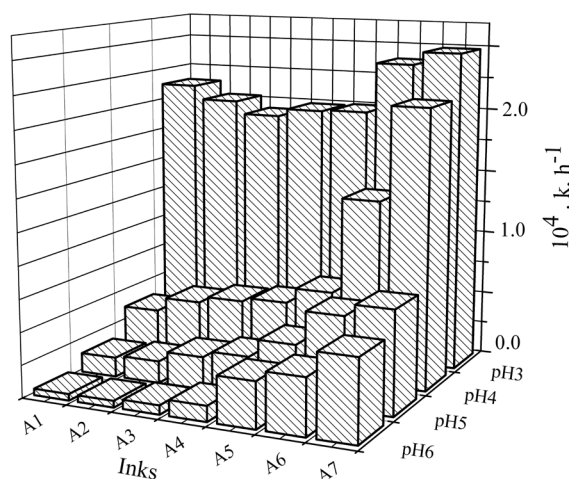


Fig. 1. Rate constants of degradation vs. ratio Cu:Fe (A1–A7) and pH

The rate constants of degradation are significantly higher at the pH value around 3, the ratio Cu:Fe in inks does not significantly affect the rate of degradation. With increasing pH the rate of degradation descends and depends on the ratio Cu:Fe in inks. Samples with higher content of copper in the inks exhibit higher constant of degradation at the same pH value.

The color changes of selected samples during ageing are on the Fig. 2.

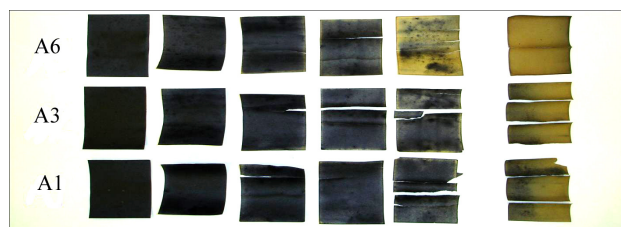


Fig. 2. Samples of inks (A1, A3, A6) at the ageing time of 0, 1, 2, 3, 4 and 24 hours, pH 3

The colorimetric changes of the samples during ageing can be summarize as follow. CIE Lab lightness of samples aged at the pH range 3 increases with prolonged ageing and this bleaching is steepest for the samples with higher content of copper (Figs. 3–5.). At the same time CIE Lab chroma increases from small initial values (1.8) to the values up to 20 and CIE Lab hue angle is shifted from 280° to 76° (corresponds to the shift from grey to brown-yellowish color). More significant changes of chroma and hue angle during ageing were observed for the samples with higher content of cooper. The nature of these changes suggests that oxidative reactions of the iron-gall ink take place in addition to the degradation of cellulose fibers.

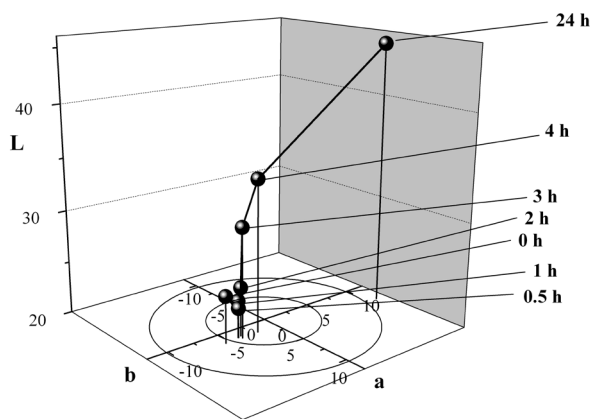


Fig. 3. Changes of colorimetric parameters (CIELab) during ageing; sample A1, pH 3

Colorimetric changes of samples aged in higher pH ranges follow the above trend, but were less significant (color difference $DE_{ab}^* < 3.5$). Lower extend of changes of color corresponds to the lower rate of degradation in these pH ranges

In order to asses the role of hydrolytic degradation and the catalytic influence of transitional metals, the rate constants of degradation of pure substrate (Whatman paper) without ink deposition at various pH were determined (Fig. 6.).

As follows from the Figs. 6 and 7., the degradation of the samples containing iron gall inks is significantly higher than the degradation of samples of the pure substrate

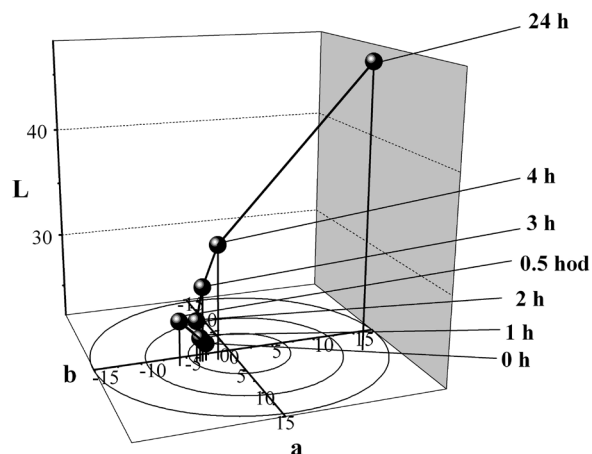


Fig. 4. Changes of colorimetric parameters (CIELab) during ageing; sample A3, pH 3

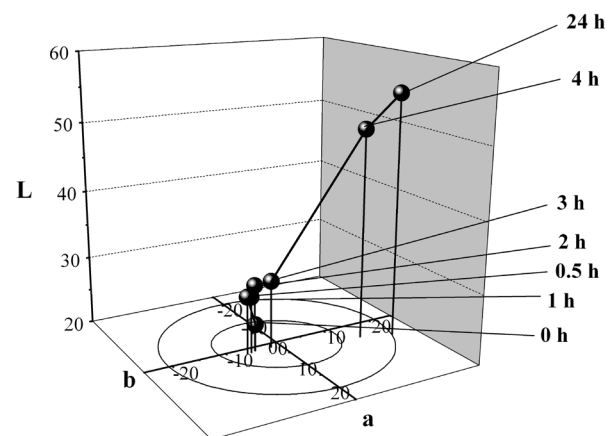


Fig. 5. Changes of colorimetric parameters (CIELab) during ageing; sample A6, pH 3

of the same pH. While the increasing of pH value of pure substrate to 3 increased the rate constant of degradation about 4-times, the change of pH value from 6 to 3 for the sample with ink A1 increased the rate constant of degradation about 20-times. This can be considered as evidence, that the accelerated degradation of samples containing transitional metals is not caused simple by increased acidity but that specific degradation reactions of cellulose fibers catalyzed by transitional metals play significant role.

Conclusions

The rate of degradation of samples of paper with iron-gall inks containing copper and iron in various ratios is the highest at the lowest pH values (around 3) and the value of rate constant of degradation does not depend significantly on the content of cooper in the ink in this pH range. Rate of degradation of the samples in less acidic regions is lower and depends on the content of cooper. The degradation of samples

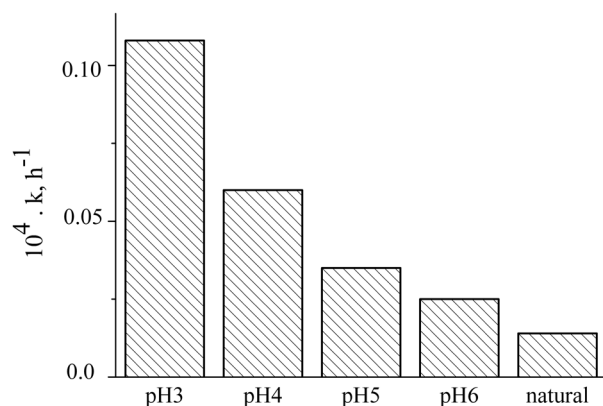


Fig. 6. Rates constants of degradation of substrate (Whatman paper) without ink deposition at various pH and without pH adjustment (natural substrate)

with inks with higher ratio copper:iron is faster, what may be caused by more significant oxidative degradation.

Accelerated degradation of samples containing transitional metals is not caused simple by increased acidity but that specific degradation reactions of cellulose fibers catalyzed by transitional metals play significant role.

Changes of colorimetric parameters during degradation of studied samples provide further indication of the running oxidation reactions.

This work was supported by Slovak Grant Agency VEGA (project VEGA 1/0800/08) and by MŠ SR (project MVTs COST D42/08 and project 2003SP200280301 Kniha SK).

REFERENCES

- Zou X., Gurnagul N., Uesaka T., Bouchard: *Polym. Deg. Stab.* 43, 393 (1994).
- Neevel J. G.: *Restaurator* 16, 143 (1975).
- Walling C.: *ACC. Chem. Res.* 8, 125 (1975).
- Wardman P., Candels L. P.: *Radiat. Res.* 145, 523 (1996).
- Bicchieri M., Pepa S.: *Restaurator* 17, 165 (1966).
- Kolar J., Strlic M.: *Acta Chim. Slov.* 50, 763 (2003).
- Wagner B., Bulska E., Hulanicki A., Heck M., Ortner H. M.: *Fresenius J. Anal. Chem.* 369, 674 (2001).
- Barb W. G., Baxendale J. H., George P., Hargrave K. R.: *Trans. Faraday Soc.* 47, 591 (1951).
- Lojzewski T., Baranski A.: *Proceedings of the International Conference Durability of Paper and Writing*, (Kolar J., Strlic M., Havermans J. B. G. A. eds.) pp. 39, Ljubljana 2004.
- ISO 5351-1:1981, *Cellulose in dilute solutions - Determination of limiting viscosity number – Part 1: Method in cupri-ethylene-diamine (CED) solution*.
- Evans R., Wallis A. F. A.: *Proceedings 4th Int. Symp. Wood Chem.* p. 201 (1987)
- Kolar J., Strlic M.: *Restaurator* 23, 94 (2004).
- Emsley A. M., Heywood R. J., Ali M., Eley C. M.: *Cellulose* 4, 1 (1997).
- ISO 13655:1996, *Graphic technology – Spectral measurements and colorimetric computation for graphic arts images*.

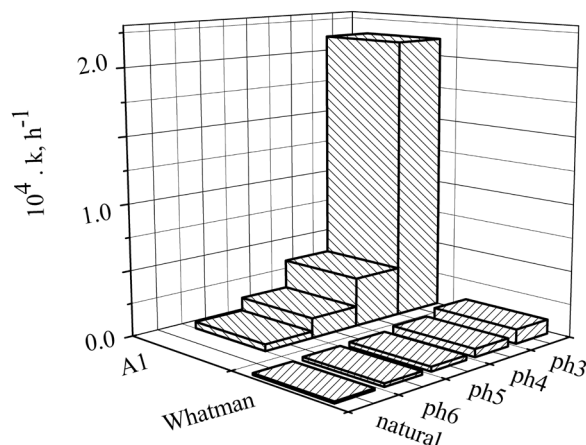


Fig. 7. Rate constants of samples from Fig. 6 compared with rate constants of degradation of sample A1

L04 PHOTOCHEMICAL TRANSFORMATION OF ANTICANCER DRUG IRINOTECAN

DANA DVORANOVÁ, VLASTA BREZOVÁ, ZUZANA VRECKOVÁ and MARIÁN VALKO

Institute of Physical Chemistry and Chemical Physics, Faculty of Chemical and Food Technology, Slovak University of Technology in Bratislava, Radlinského 9, 812 37 Bratislava, Slovak Republic, dana.dvoranova@stuba.sk

Introduction

The camptothecin family of anticancer medicines has a unique mechanism of action directed to the inhibition of topoisomerase I (Topo I). It was previously shown that camptothecin (CPT) inhibits Topo I *via* the formation of ternary complex, in which the biologically active lactone ring of CPT stabilizes an irreversible Topo I/DNA covalent complex. Camptothecin molecule contains conjugated system of π -electrons representing a potential basis for UVA photoexcitation resulting in the reactive free radical species generation (e.g., ROS – Reactive Oxygen Species), which are responsible for light-mediated DNA cleavage. Consequently, alternative mechanisms of DNA damage upon the simultaneous application of CPT, Topo I and UV radiation ($\lambda = 365$ nm) were considered. A number of photoactive compounds require the contribution of a metal ion for the DNA cleavage event, therefore the biological activity of irradiated CPT has been tested also in the presence of Cu(II) ions^{1,2}. Our previous investigations were oriented on study of interaction of CPT with Cu(II) and Fe(III) ions upon irradiation. The results obtained confirm the participation of these ions in the photoinitiated activation of camptothecin accompanied with the formation of reactive radical species^{3,4}.

Irinotecan (CPT-11 or Camptosar[®]) is a watersoluble semisynthetic analogue of the natural alkaloid camptothecin. The structure of CPT-11 is shown in Fig. 1.

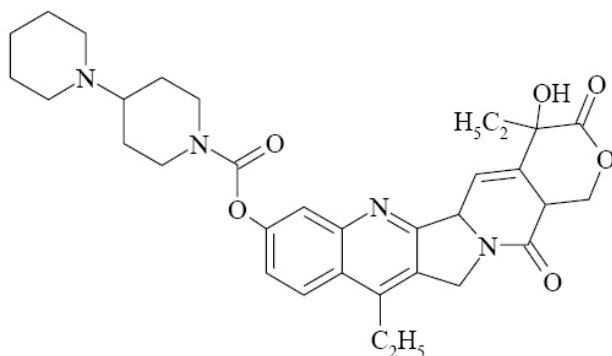


Fig. 1. Structure of irinotecan (CPT-11)

Irinotecan is a pro-drug, converted *in vivo* to its active metabolite. CPT-11 interfere with Topoisomerase I and cancer cells death appears to result from DNA strand breaks caused by the formation of cleavable complexes.

Our investigation was focused on photochemical transformations of CPT-11 in aqueous and dimethylsulfoxide (DMSO) solutions, and on its photoactivation in the presence of equimolar amounts of Cu(II) ions monitored by EPR spectroscopy.

Experimental

Irinotecan hydrochloride (CPT-11, Fig. 1) and cupric chloride were applied in photochemical experiments. 5,5-Dimethyl-1-pyrroline N-oxide (DMPO) and α -(4-pyridyl-1-Oxide)-N-*tert*-butylnitron (POBN) were used as spin trapping agents, 2,2,6,6-tetramethyl-4-piperidinol (TEM-POL) was applied as spin label. The selective oxidation of 4-hydroxy-2,2,6,6-tetramethylpiperidine (TMP) *via* singlet oxygen to the paramagnetic nitroxyl radical oxyl (TEMPOL) was utilized for $^1\text{O}_2$ detection by EPR spectroscopy.

The stock solutions of CPT-11 and CuCl_2 (both 2×10^{-3} mol dm^{-3}) were prepared in redistilled water or dimethylsulfoxide. The CPT-11 (150 μl) were mixed with identical volume of solvent (water or DMSO) or 150 μl Cu(II) ions (to obtain equimolar solution CPT-11: Cu(II)) and 50 μl of aqueous or DMSO solutions of spin traps/spin label were added prior to irradiation. The prepared solutions were saturated by argon or air, filled in the quartz flat cell optimized for the Bruker TE₁₀₂ EPR cavity.

The X-band EPR spectra were recorded at EPR Bruker EMX spectrometer equipped with a TE₁₀₂ (ER 4102ST) resonator. Samples were irradiated at 295 K *in situ* using HPA 400/30S lamp (400 W, $\lambda_{\text{max}} = 365$ nm, Philips, UVA irradiance 10 mW cm^{-2}). A Pyrex glass filter was applied to eliminate the radiation wavelengths below 300 nm. The simulations of the individual components in the complex EPR spectra were calculated using WinEPR and SimFonia programs (Bruker). The experimental EPR spectra were fitted as the linear combinations of these individual simulations using a least-squares minimization procedure with the Scientist Program (MicroMath).

Results

The EPR spin trapping technique enables to evidence reactive short-lived free radicals adding them to spin trapping agent under the formation of more stable paramagnetic products (spin adducts). The EPR spectrum of adducts brings information on type of reactive radical trapped.

DMPO. The dimethylsulfoxide solvent is well known for its ability to stabilize super-oxide anion radical. The EPR spectra measured after 10 min of irradiation of CPT-11 in DMSO solutions under air in the presence of DMPO confirmed the formation of two radical adducts (Fig. 2.). The spin Hamiltonian parameters of EPR signals obtained by simulation analysis revealed the generation of $^{\bullet}\text{DMPO-O}_2^-$, characterized by hyperfine splittings $a_{\text{N}} = 1.274$ mT, $a_{\text{H}}^{\beta} = 1.035$ mT, $a_{\text{H}}^{\gamma} = 0.137$ mT and g -value = 2.0058(ref.⁵). This EPR signal dominates in the experimental spectrum (relative concentration 80 %), and is produced immediately after beginning of irradiation. Additionally, a minor EPR signal was

observed, attributed to $\cdot\text{DMPO-OCH}_3$ adduct ($a_N = 1.330$ mT, $a_H^\beta = 0.794$ mT, $a_H^\gamma = 0.155$ mT and g -value = 2.0058)⁵.

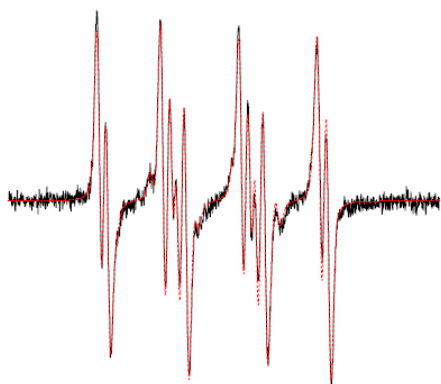


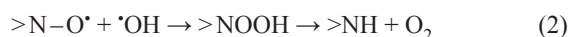
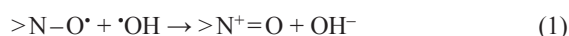
Fig. 2. Experimental (solid line) and simulated (dotted line) EPR spectra (magnetic field sweep 7.5 mT) obtained after 10 minutes of a continuous irradiation of system CPT-11/DMPO/DMSO/air. Initial concentration: $c_0(\text{CPT-11}) = 0.86$ mmol dm⁻³ and $c_0(\text{DMPO}) = 30$ mmol dm⁻³

The formation of superoxide anion radicals upon photoexcitation of CPT-11 in DMSO solvent was unambiguously confirmed by the addition of enzyme superoxide dismutase (SOD) into the solution, which caused a significant decrease of $\cdot\text{DMPO-O}_2^-$ EPR intensity by the competitive reaction of SOD with $\text{O}_2^{\cdot-}$.

The production of $\cdot\text{DMPO-OCH}_3$ adduct was established previously in aerated DMSO systems producing oxygen-centered free radicals ($\text{O}_2^{\cdot-}$, $\cdot\text{OH}$). Probably, the generation of this minor adduct reflected the reaction of ROS with solvent producing $\cdot\text{CH}_3$ radicals, which are in the presence of molecular oxygen transformed to $\text{CH}_3\text{OO}\cdot$ and trapped as $\cdot\text{DMPO-OCH}_3$.

It should be noted here that the application of DMPO was not possible in systems containing Cu(II) ions and DMSO solvent, due to the formation of paramagnetic species even after mixing of individual solutions before irradiation, so the identification of photo-induced radical adducts was limited.

TEMPOL. The principle of the detection of reactive free radical formation using TEMPOL and its derivatives is based on monitoring the decrease in its EPR intensity resulting from the interaction of its $>\text{N-O}\cdot$ group with the generated reactive radical species, as well as singlet oxygen (Eqs. 1–4)⁶:



The EPR spectrum of TEMPOL in DMSO solvent in the presence of oxygen represents three-line signal characterized with hyperfine splitting $a_N = 1.573$ mT and $g = 2.0060$, as il-

lustrates inset in Fig. 3.a. Irradiation of TEMPOL in DMSO solution under air or argon confirmed its photochemical stability under air or argon confirmed its photochemical stability under experimental conditions, as only negligible decrease of EPR signal was observed. The situation was similar if TEMPOL was irradiated in the presence Cu(II) ions. However, the addition of CPT-11 to the reaction system under air or argon led to the decrease of TEMPOL signal.

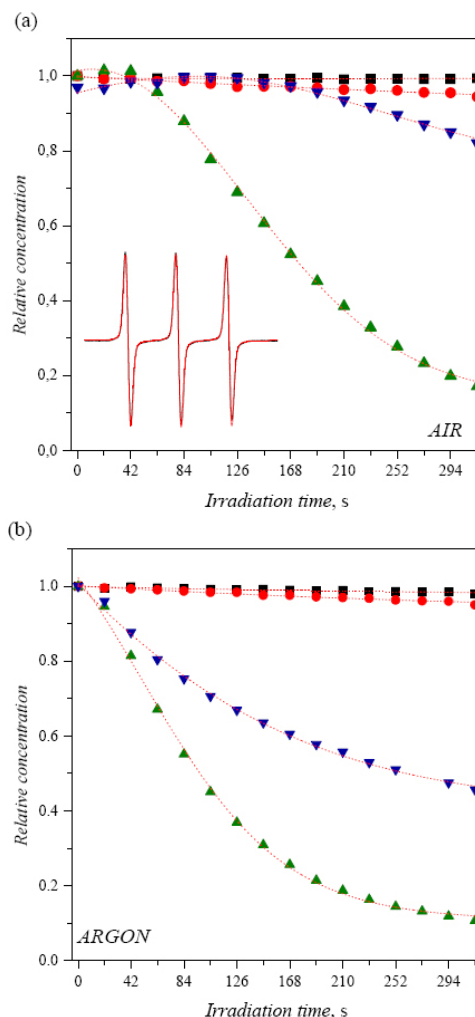
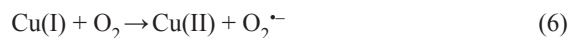


Fig. 3: TEMPOL relative concentration monitored upon continuous irradiation ($\lambda > 300$ nm) of DMSO solutions in the presence CPT-11 and/or Cu(II) ions ($c_0(\text{TEMPOL}) = 43$ $\mu\text{mol dm}^{-3}$) under air (a) and argon (b). Inset represents experimental and simulated EPR spectrum of TEMPOL in DMSO (magnetic field sweep 6 mT). Initial concentrations of CPT-11 and Cu(II) ions (in mmol dm⁻³): ■ $c_0(\text{CPT-11}) = 0$, $c_0(\text{Cu(II)}) = 0$; ● $c_0(\text{CPT-11}) = 0$, $c_0(\text{Cu(II)}) = 0.86$; ▲ $c_0(\text{CPT-11}) = 0.86$; $c_0(\text{Cu(II)}) = 0$; ▼ $c_0(\text{CPT-11}) = 0.86$, $c_0(\text{Cu(II)}) = 0.86$

The addition of equimolar amount of Cu(II) ions into CPT-11 solution and subsequent irradiation led to the decrease of TEMPOL signal which was less pronounced than in system with only CPT-11.

The termination of TEMPOL signal in the presence of CPT-11 indicated the formation of reactive radical species which can react with TEMPOL, forming diamagnetic products. The presence of Cu(II) ions in reaction systems with CPT-11 could cause the competitive reactions, e.g., reoxidation of Cu(II) (Eqs 5, 6):



Additionally, the formation of singlet oxygen $^1\text{O}_2$ was confirmed, as irradiation of CPT-11 in the presence of TMP resulted to the formation of TEMPOL radical.

Conclusions

The work was focused on spectroscopic characterization of photoinitiated processes of irinotecan. Radical formation in the photoactivated system with CPT-11 and CPT-11/Cu(II) was monitored by spin traps DMPO and POBN under inert atmosphere and also in the presence of oxygen. DMPO was used for confirmation of photoinduced reactive radical species formation in DMSO solutions and POBN in aqueous solutions, respectively. Semi-stable free radical TEMPOL was used to verify the production of radicals upon irradiation.

Dedicated to Prof. Andrej Staško on the occasion of his 70th birthday.

This study was financially supported by Scientific Grant Agency of the Ministry of Education of the Slovak Republic (Projects VEGA 1/3579/06) and Research and Development Agency of the Slovak Republic (contract No. APVV 0055-07).

REFERENCES

1. R. P. Hertzberg, M. J. Caranfa, S. M. Hecht, *Biochem.* 28, 4629 (1989).
2. S. M. Hecht, *Curr. Med. Chem. Anti-Cancer Agents* 5, 353 (2005).
3. V. Brezová, M. Valko, M. Breza, H. Morris, J. Telser, D. Dvoranová, K. Kaiserová, E. Varečka, M. Mazúr, D. Leibfritz, *J. Phys. Chem. B* 107, 2415 (2003).
4. D. Dvoranová, V. Brezová, M. Valko, A. Staško *J. Photochem. Photobiol. A: Chem.* 185, 172 (2007).
5. A. S. W. Li, K. B. Cummings, H. P. Roethling, G. R. Buettner, C. F. Chignell, *J. Magn. Reson.* 79, 140 (1988). (The database is available at <http://epr.niehs.nih.gov>).
6. V. Brezová, S. Gabčová, D. Dvoranová, A. Staško *J. Photochem. Photobiol. B: Biol.* 79 121 (2005).